Review Paper

SQUID multiplexers for transition-edge sensors

K.D. Irwin
Mail Stop 814.03
National Institute of Standards and Technology
325 Broadway
Boulder, CO 80305-3328

SQUID multiplexers for transition-edge sensors[†]

K.D. Irwin [a]

a. NIST, Boulder, CO, USA

Abstract

We review the SQUID multiplexer schemes that are being developed to instrument large-format arrays of superconducting transition-edge sensors. We discuss the choice of an orthogonal basis set to represent the multiplexed signal (such as time or frequency) and the practical issues of implementation, including bandwidth-limiting filters, SQUID noise, and power dissipation.

Keywords: SQUID; Multiplexer; Transition-edge sensor

1. Introduction

Microcalorimeters and bolometers based on superconducting transition-edge sensors (TES) are important tools for the detection of photons from millimeter waves through the x-ray, and for applications ranging from materials analysis to astronomy. The low noise, low power, and low impedance of Superconducting Quantum Interference Devices (SQUIDs) make them the preamplifier of choice for TES devices. Due to constraints on wiring and circuit complexity, SQUID multiplexing is necessary to instrument large-format arrays.

First-generation SQUID multiplexers have now been deployed in small arrays. We review the state of the art in SQUID multiplexers for TES detectors.

2. Multiplexing TES detectors

TES detectors have two properties that limit the appropriate multiplexer schemes. First, the response of a TES detector is rolled off at the thermal-response frequency, but the total noise (phonon + Johnson) is wideband and close to white for an ideal, voltage-biased detector [1]. It is thus important to implement a filter, since only bandwidth-limited signals can be multiplexed without degradation. Second, TES detectors have significant noise in the absence of signal (dark current noise). Thus, multiplexing schemes that irreversibly add the noise from different TES detectors will degrade the signal-to -noise ratio (SNR).

A variety of TES SQUID MUX schemes have been proposed that accept SNR degradation due to the absence of a bandwidth-limiting filter [2], or due to the irreversible mixing of noise from different pixels. While these approaches may be useful in some cases (e.g., when photon noise dominates), we focus here on two multiplexing approaches that maintain the SNR: time-division multiplexing (TDM) and frequency-division multiplexing (FDM).

2.1 Information content and multiplexing

According to the Nyquist theorem, the information in a signal of bandwidth δf and duration δt can be exactly represented by $2\delta f \delta t$ real samples in time space. The same signal can be represented in frequency space as a Fourier series with $2\delta f \delta t$ real samples. The time and frequency samples form orthogonal basis sets to represent the bandwidth-limited function. Any basis set can be used for the representation. It is convenient that the basis set be orthogonal. Further, if an output SQUID channel has a bandwidth δF (larger than the signal bandwidth δf) it is possible in principle for the output to carry $M \le \delta F / \delta f$ signals without degradation in M

different subsets of the output basis set.

In order to multiplex, the bandwidth of the signal is limited by a filter, the information in each signal is moved to a different subset of the output basis set (the signal is 'encoded'), and the signals are summed in the output channel. The signals are encoded by multiplying them by a set of orthogonal modulation functions. The multiplication can be done in either the TES or the SQUID. In TDM, boxcar (low-duty-cycle square-wave) modulation functions are used. In FDM, a sinusoid is used. The signals are then added into one output channel. They can be separated and decoded using the same modulation functions.

In the absence of SQUID noise, the fundamental limit on the number of signals that can be encoded in one output channel with a given bandwidth is independent of the choice of orthogonal basis set.

The bandwidth required for single TES microcalorimeters and bolometers in most applications is 0.1 to 10 kHz. It is possible in principle to multiplex 32 channels in the bandwidth of several MHz available with SQUIDs linearized with feedback from room-temperature circuits.

2.2 SQUID noise and multiplexing

Wideband SQUID noise is added to the signals after they are encoded. During decoding, all the noise outside the noise bandwidth of the encoded signal is filtered out. The amount of noise that is added to the decoded signal depends on the noise bandwidth of the encoded signal. We assume here that the noise is white.

In TDM, the bandwidth of the encoded signal is set by the boxcar modulating function. In frequency space, the boxcar function is a sinc function, $F_{\mathrm{mod}}(f) = \sin(\pi f \delta t_s)/(\pi f \delta t_s)$, where δt_s is the time that the multiplexer dwells on one pixel. The noise bandwidth of the sinc function is

$$\int_0^\infty \left(\frac{\sin(\pi f \delta t_s)}{\pi f \delta t_s} \right)^2 df = 1/2\delta t_s . \qquad (1)$$

The noise above this noise bandwidth is filtered by the sinc function in the process of decoding, either in an analog circuit (a gated integrator), or digitally, by averaging an oversampled signal. The 'frame rate,' $1/(M\delta t_s)$, is the rate at which all pixels are sampled. All the unfiltered noise above $1/(2M\delta t_s)$, the Nyquist frequency associated with the frame rate, is aliased into the signal band. The effective noise power of the SQUID is thus increased by a factor of $2M\delta t_s/2\delta t_s = M$. In order to maintain fixed SNR, the gain must be $\sqrt{M}$ times larger than it would be for a non-multiplexed TES: the number of turns on the input coil must be increased. Note that SQUIDs are sufficiently quiet that, even with the required gain, it is possible in principle to multiplex hundreds of signals in one output SQUID with TDM [3].

In FDM, in contrast, the bandwidth of the encoded signal is the same as the bandwidth of the input signal. Multiplying by the modulating function, a sinusoid, moves the signal up to a high frequency, but does not affect the bandwidth. Thus, no aliasing of wideband noise occurs. However, coupling multiple pixels to the SQUID in FDM can decrease the coupling efficiency to the SQUID. At least for some coupling schemes, this effect can impose a similar $\sim\sqrt{M}$ increase in the required gain, as will be discussed later.

3. SQUID MUX implementations

In both the TDM and the FDM schemes described here, two-dimensional arrays of TES detectors with dimensions $M \times N$ are multiplexed columnwise with M orthogonal modulating functions and N output SQUIDs.

3.1 Time-division SQUID multiplexing

Early in the development of voltage-biased TES detectors, it was suggested that they could be time-division multiplexed with SQUIDs [4]. In TDM, each TES is instrumented by a separate first-stage SQUID. M boxcar modulation functions are applied by sequentially turning on the first-stage SQUIDs in a column. The bandwidth of the TES is limited by a one-pole low-pass L/R filter formed by the inductance of the SQUID's input coil (and possibly an extra inductor) and the resistance of the TES.

In TDM (but not in FDM), the signal must be filtered before it is multiplied by the modulation function, since the low-pass filter rolls off at frequencies below the bandwidth of the sinc function. Thus, the TES cannot be used as the modulating element without SNR degradation.

In first-generation "parallel-address" SQUID TDM, the modulation function was applied to the first-stage SQUIDs by applying an address *voltage* in *parallel* to the address resistors to turn on a row of SQUIDs [3]. However, in improved "series address" designs [5], boxcar address *currents*, $I_1(t)$, $I_2(t)...I_M(t)$, are applied to turn on a row of M first-
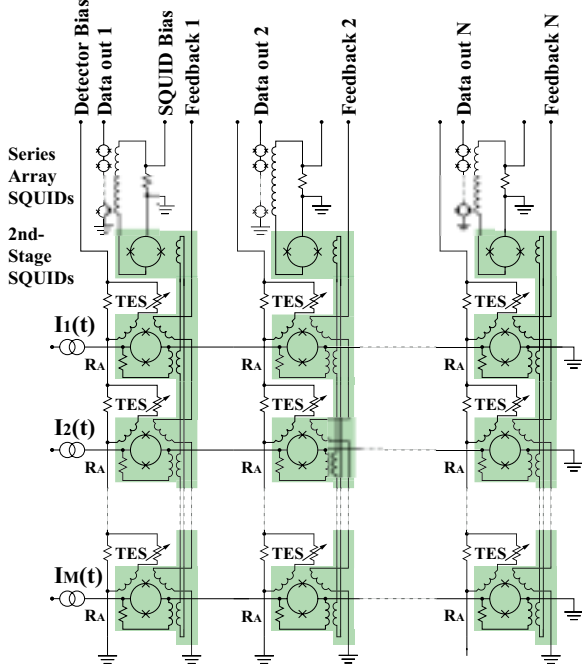
Fig. 1. Circuit diagram for time-division SQUID multiplexer with M×N pixels. In this version, the first-stage SQUIDs are coupled through a common transformer to the second stage.

stage SQUIDs in *series* (Fig. 1). A ~1 Ω address resistor, R_A, shunts each first-stage SQUID. The current through the address resistor is inductively coupled to a second-stage SQUID shared by all the first-stage SQUIDs in a column. The coupling to the second stage can occur either through a transformer coil that is common to all of the first-stage SQUIDs (Fig. 1) or through separately wound input coils from each channel to the second-stage (not shown).

A feedback flux is provided to the switched first-stage SQUIDs to linearize them. Since only one SQUID in a column is on at a time, one feedback coil can be common to all SQUIDs in the column (Fig. 1). At high switching rates, inductive coupling from the common feedback coil to the input coil can be a source of crosstalk between the 'on' channel and all of the 'off' channels in the column. The inductive coupling is canceled by connecting each TES to the input coils of two SQUIDs with oppositely wound feedback coils. Only one SQUID of the pair is turned on. This 'balanced pair' configuration (Fig. 2) geometrically nulls the coupling between the feedback coil and input coil.

The feedback is applied by room-temperature electronics that have an analog-to-digital converter (ADC), a field-programmable gate array (FPGA), and a digital-to-analog converter (DAC) for each multiplexed column. When the SQUID associated with a pixel is on, its output is measured by the ADC.
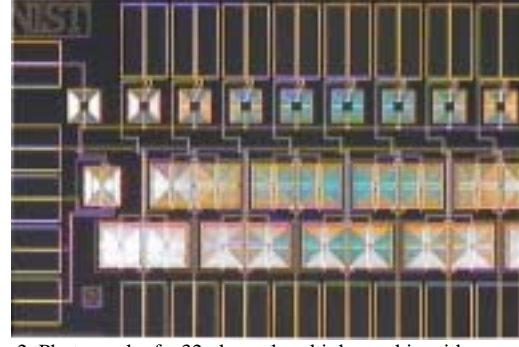

Fig. 2. Photograph of a 32-channel multiplexer chip with transformer coupling to the second stage. The second stage and about 8 of the 32 channels is shown. A 'balanced pair' of two SQUIDs are seen at each input channel.

The appropriate feedback signal to null the flux of the 'on' SQUID is applied by the DAC to the common feedback coil. When the SQUID is turned off, the value of the DAC voltage required to null the SQUID flux is stored in the FPGA; the next time the pixel is turned on, the feedback algorithm is continued from the previous value of flux.

First-generation 8-pixel SQUID MUX chips have been used to instrument 8-pixel TES bolometers by the Goddard and NIST groups. SQUID TDM has been shown to operate without significantly contributing to the noise of the bolometer [6]. Fig. 3 shows the demultiplexed response of the array to a chopped optical load. The bolometer array has been deployed in a submillimeter Fabry-Perot spectrometer, FIBRE, at the Caltech Submillimeter Observatory and used in initial astronomical observations [7]. Second-generation 32-pixel series-address MUX chips (Fig. 2) have now been fabricated by the NIST group [5].
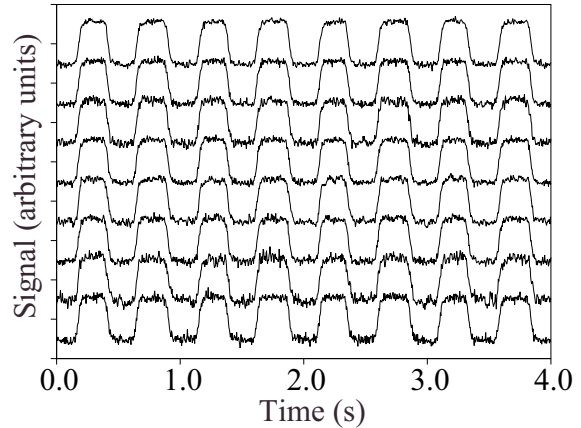

Fig. 3. The response of a time-division multiplexed 8-pixel TES bolometer array to a chopped optical load. The SQUIDs are linearized by switched digital feedback, and the 8 channels are demultiplexed in the figure.

SQUID TDM will be used in a 1000-pixel x-ray microanalysis array being developed at NIST, in SAFIRE [8], a 288-pixel first-light instrument on SOFIA, and in SCUBA-2 [9], a 12,800-pixel submillimeter bolometer array to be deployed at the James Clerk Maxwell Telescope in ~2005. It is also being developed as an option for NASA's x-ray observatory, Constellation-X [10].

Finally, it may be possible to implement SQUID TDM using digital SQUIDs [11], or SQUIDs with local feedback and outputs modulated and summed by a cryogenic CMOS multiplexer [12]. Significant reduction in the power dissipation would be required to make digital SQUIDs practical for this application. Because of their high speed and high power dissipation, a SQUID/CMOS MUX might be useful in applications requiring arrays of modest size, but with high bandwidth at each pixel, such as high-count-rate TES x-ray microcalorimeters or TES optical detectors.

3.2 Frequency-division SQUID multiplexing

In FDM, the TES is used as the modulating element [13,14,15]. The M sinusoidal modulation functions, $I_1(t)$, $I_2(t)...I_M(t)$, are applied either to bias resistors for each TES element, or to transformers that provide a sinusoidal voltage bias to each TES element (Fig. 4). The TES signal is thus moved up to a frequency band around the carrier signal. After encoding, the bandwidth of the signal is limited by an LCR tank filter formed by a tuned inductor and capacitor at each pixel and the resistance of the TES (Fig. 4). The frequency of the passband is $1/\sqrt{LC}$ and the bandwidth is $2\pi R/L$ (in the narrow-band limit).

The current through the TES is coupled to an output SQUID either through a transformer 'summing' coil [13] that is common to all the first-stage SQUIDs (Fig.4), by wiring the TES detectors in parallel [14,15] so that all of the signal currents flow through a common SQUID coil (not shown), or by connecting each TES to a separately wound input coil to the SQUID (not shown). If a summing coil is used, a feedback flux is applied to the coil to linearize the SQUID and reduce crosstalk. If the TES detectors are wired in parallel, a feedback current is applied to keep the total current through the common SQUID coil fixed, linearizing the SQUID and reducing crosstalk. If the TES detectors are wired to separate input coils, a feedback flux is provided to the SQUID.
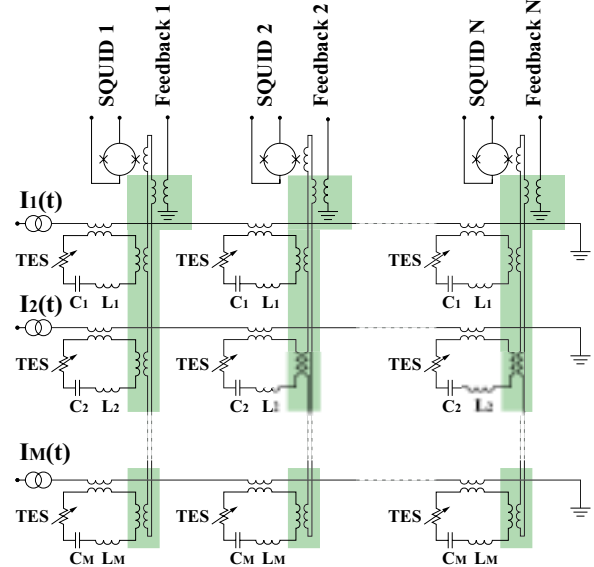

Fig. 4. Circuit diagram for frequency-division SQUID multiplexer with M×N pixels. In this version, the TES detectors are coupled through a summing coil to the SQUID, and a transformer applies the detector bias voltages.

If the coupling to the SQUID is through a summing coil, coupling inefficiency increases the SQUID current noise referred to the transformer coil primary by $\sqrt{2M}$ for a fixed SQUID flux noise [13]. Note that SQUIDs are sufficiently quiet that, even with the additional noise, it is possible in principle to multiplex hundreds of signals in one output SQUID with a summing coil [13]. Other coupling schemes may have an advantage in coupling efficiency, although the analysis is not yet complete [16].

The Berkeley group has fabricated [13] 8-pixel summing coils for SQUID FDM (Fig. 5a). Eight carrier signals of different frequencies were injected into the coils and read out with a commercial SQUID system, demonstrating the summing of the simulated input signals into the output SQUID (Fig. 5b). Individual carrier signals were selected with a lock-in amplifier to demonstrate demultiplexing. Work is underway to connect the summing coils to TES detectors, and to implement LC filters to limit the bandwidth of the signals.

A technical challenge facing SQUID FDM is the implementation of practical LC filters with center frequencies convenient for SQUID readout. Inductances of a few microhenries are readily achievable with lithographic superconducting coils in typical pixel areas of ~1 mm. To operate with LC filters at the most convenient frequency band of <~ 1 MHz would require large capacitors (>~ 10 nF) that may prove difficult to fabricate. To operate at these
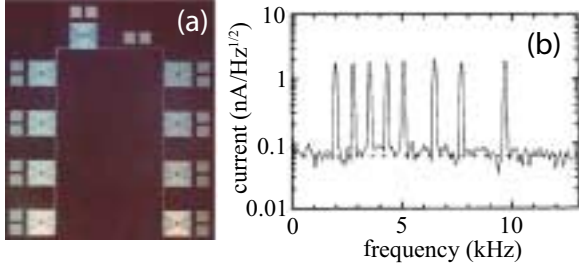
Fig. 5. (a) Photograph of an 8-pixel summing coil for SQUID FDM. The feedback coil and output bond pads are on the top. (b) Power spectral density of the feedback current for a SQUID connected to the 8-pixel summing coil. Shunt resistors are connected across each input, and eight carrier signals are injected at eight different frequencies to simulate signals. The dotted line indicates the quadrature sum of the Johnson noise from the 8 resistors. Figure courtesy of J. Yoon.

low frequencies, it is necessary to use either component capacitors connected to every pixel, or to use very thin dielectrics or materials of high dielectric constant (such as $SrTiO_3$). It has been suggested that a process similar to the standard niobium trilayer could be used to fabricate a capacitor with a very thin Al_2O_3 barrier over a large area [18]. The challenge is to cover large areas (~1 mm^2 per pixel) with no pinholes.

Alternatively [17], a multiplexer could be designed to operate with high-bandwidth SQUIDs (>~ 25 MHz) using currently available, high-yield lithographic capacitor processes. Because of cable delays, this bandwidth is too high for feedback to be provided from room-temperature electronics. The SQUID could be operated open-ended, or feedback could be provided locally (e.g. digital SQUIDs [11], or a series-array SQUID op-amp [12]), or from a cooled semiconductor amplifier at an intermediate temperature stage [18].

Another challenge facing FDM is to develop SQUIDs with high enough slew rates to handle the combined sinusoidal carrier signals from all multiplexed pixels. The application of a flux signal to the SQUID to buck the equilibrium carriers may make this easier to achieve.

SQUID FDM is being developed for submillimeter astronomy [13], for x-ray applications [19], and for the European Space Agency's XEUS x-ray observatory [17].

3.3 Technical tradeoffs

There are a variety of technical tradeoffs that should be considered in choosing the optimal scheme for multiplexing large arrays of TES detectors for a particular application. These tradeoffs include the

efficiency of bandwidth usage, the complexity of room-temperature electronics, the difficulty of connecting detectors to SQUIDs, the power dissipation, the effect of SQUID noise, and the difficulty of constructing bandwidth-limiting filters.

The limits on the efficiency of bandwidth utilization are similar for the TDM and FDM schemes that have been described here. In TDM, dead time due to switching transients reduces the number of channels that can be multiplexed in the available bandwidth. Since SQUIDs settle on the short timescales of Josephson oscillations, the switching transient time is limited by the slowest time constant in the rest of the system. Similarly, in FDM the frequency spacing between the adjacent channels that is necessary to reduce crosstalk limits the number of channels that can be multiplexed. In TDM, the one-pole L/R filter used to limit the pixel bandwidth must have a knee frequency $3 + 2\sqrt{2} \approx 5.8$ times higher than thermal response bandwidth in order for the detector's operation to be stable [20]. Similarly, in FDM, the passband must be ≈ 5.8 times wider than the thermal response bandwidth [17]. When all of these factors are taken into account, the efficiency of bandwidth utilization in each case is similar.

TDM requires complex electronics due to the switched digital feedback needed to linearize the SQUIDs. Custom electronics is required, although components with sufficient performance are commercially available.

FDM requires complex electronics to simultaneously demodulate the signals in all of the passbands. A dedicated analog circuit for each pixel could be used for the demodulation, but this approach would be difficult for very large arrays. A column of detectors can also be instrumented with an ADC and digital-signal processor (DSP) to digitally demodulate all signals simultaneously. Demodulation with sinusoids is computationally intensive. It will be challenging both to develop the fast room-temperature electronics for the application and to fit them into the power specifications of a satellite mission, especially for higher frequency systems.

FDM has an advantage in its lead requirements, since it may be easier to integrate passive inductors and capacitors on the same wafer with TES detectors than it is to integrate active SQUID components. If the LC filters are on the same wafer as the detectors, the number of leads that will have to be pulled off the wafer is significantly reduced. Note however that ~100x100 arrays of bump bonds are routinely

fabricated for IR detectors [21].

In both FDM and TDM, one or two SQUIDs are on per column, dissipating ~ 1 μW of power in the first stage for a 32×32 array. This power is acceptable at the base temperature for many applications, but in instruments with extremely low power budgets it may be necessary to place the SQUIDs at a higher temperature. This would take fewer leads in FDM than in TDM.

As discussed in section 2.2, aliased out-of-band SQUID noise makes the gain required to maintain fixed SNR in TDM larger than in FDM by a factor of $\sqrt{M}$. Also, as described in section 3.2, the use of a summing coil makes the required gain in FDM larger by a factor of $\sqrt{2M}$ and similar decreases in coupling efficiency may or may not occur for other FDM coupling schemes. The larger gain leads to an increase in the self-inductance of the SQUID input coil, and hence to a decrease in the highest frequency response of the detectors. From eqn. 2 of reference [3], the maximum frequency response, f, of a multiplexed TES detector is limited by the SQUID noise requirement to

$$f \leq \frac{4}{3 + 2\sqrt{2}} \frac{k_B T \alpha^2 L_{squid}}{\gamma S_\Phi \pi} \, , \qquad (2)$$

where k_B is the Boltzmann constant, T is the temperature of the TES, α is the coupling constant between the input coil and the SQUID, L_{squid} is the inductance of the SQUID, S_Φ is the power spectral density of the flux noise of the SQUID, and γ is the factor by which the low-frequency detector current noise power spectral density is required to exceed the input current noise power spectral density of the SQUID. Although this equation was derived for TDM, it holds also for FDM, since the stability condition, $f_{L/R} > 5.8 f$, is the same. A different value of γ is chosen to compensate for the different gain requirements in the three cases. For instance, if the gain is required to be high enough that the SQUID noise degrades the detector noise by no more than ~15 %, then $\gamma \sim 3*M$=100 for TDM, and $\gamma \sim 3*(2M) = 200$ for FDM with a summing coil. For a 32×32 multiplexed array of TES detectors operated at T=100 mK, with typical values for SQUIDs of $S_\Phi \approx \left(1\mu\Phi_0 / \sqrt{Hz}\right)^2$, L_{squid}=20pH, and $\alpha = 0.9$, the limitation on the signal bandwidth imposed by SQUID noise is 12 kHz for TDM, and about 6 kHz for FDM with a summing coil. A similar analysis needs to be done for FDM with other coupling schemes that may have an advantage in coupling

efficiency. Note that an x-ray microcalorimeter array with a live count rate of 1000 cps per pixel requires a signal bandwidth of about 3 kHz [22]. It is likely that the practical limit on the signal bandwidth will be set by something other than the SQUID noise for applications in the near future.

Finally, as discussed in section 3.2, it is significantly easier to make low-frequency, lithographic L/R low-pass filters for SQUID TDM than it is to make low-frequency, lithographic LC filters for FDM.

Each multiplexing approach has different advantages. The details of specific instruments and the resources available will determine the optimal choice of a multiplexing technique.

References

[1] K.D. Irwin, Appl. Phys. Letters 66, 1998-2000 (1995).
[2] B.S. Karasik, W.R. McGrath, Proceedings of the 12th International Symposium on Space THz Technology, San Diego, CA, February, 2001.
[3] J.A. Chervenak, K.D. Irwin, E.N. Grossman, J.M. Martinis, C.D. Reintsema, M.E. Huber, Appl. Phys. Letters 74, 4043-4045 (1999).
[4] E.N. Grossman, personal communication 1995.
[5] K.D. Irwin, L.R. Vale, N.E. Bergren, S. Deiker, E.N. Grossman, G.C. Hilton, S.W. Nam, C.D. Reintsema, D.A. Rudman, Proceedings of the 9th International Workshop on Low Temperature Detectors, Madison, WI, July 2001.
[6] J.G. Staguhn, C.A. Allen, D.J. Benford, J.A. Chervenak, M.M. Freund, S.A. Khan, A.S. Kutyrev, S.H. Moseley, R.A. Shafer, S. Deiker, E.N. Grossman, G.C. Hilton, K.D. Irwin, J.M. Martinis, S.W. Nam, D.A. Rudman, D.A. Wollman, Proceedings of the 9th International Workshop on Low Temperature Detectors, Madison, WI, July 2001.
[7] D.J. Benford, C.A. Allen, J.A. Chervenak, M.M. Freund, E.N. Grossman, K.D. Irwin, A.S. Kutyrev, J.M. Martinis, S.H. Moseley, S.W. Nam, C.D. Reintsema, R.A. Shafer, J.G. Staguhn, Int'l J. IR MM Wave 21(12) (2000) 1909-1916.
[8] R.A. Shafer, S.H. Moseley, P.A.R. Ade, Benford, G. Bjoraker, E. Dwek, D.A. Neufeld, F. Pajot, T.G. Phillips, G.J. Stacey, Proc. SPIE 4014 (2000) 98-108.
[9] W.D. Duncan, W. Holland, D. Audley, D. Kelly, T. Peacock,P. Hastings, M. MacIntosh, K.D. Irwin , S.W. Nam, G.C. Hilton, S. Deiker, A. Walton , A. Gundlach, W. Parkes, C. Dunare, P.A.R.

Ade , I. Robson, Proceedings of the 9th International Workshop on Low Temperature Detectors, Madison, WI, July 2001.

[10] C. K. Stahle, S. Bandler, T.W. Barbee, J.W. Beeman, R.P. Brekosky, B. Cabrera, M. Cunningham, S. Deiker, E. Figueroa-Feliciano, F.M. Finkbeiner, M.A. Frank, K.C. Gendreau, E. Haller, G.C. Hilton, K.D. Irwin, Proc. SPIE 3765 (1999) 82.

[11] Radparvar, M., IEEE Trans. Superc., 4 (1994) 87.

[12] K.D. Irwin, M.E. Huber, IEEE Trans. Appl. Supercond. 11 (2001) 1265.

[13] J. Yoon, J. Clarke, J.M. Gildemeister, A.T. Lee, M.J. Myers, P.L. Richards, J.T. Skidmore, Appl. Phys. Letters 78 (2001) 371.

[14] J.J. Bock, personal communication, 1997.

[15] Miyazaki, T., PhD thesis, ISAS/Univ. Tokyo (2001).

[16] P. de Korte, personal communication (2001).

[17] M. Kiviranta, H. Seppa, J. van der Kuur, P. de Korte, Proceedings of the 9th International Workshop on Low Temperature Detectors, Madison, WI, July 2001.

[18] A.T. Lee, M. Kiviranta, personal communication 2001.

[19] M.F. Cunningham, J.N. Ullom, T. Miyazaki, O.Drury, A. Loshak, M.L. van den Berg, and S.E. Labov, Proceedings of the 9th International Workshop on Low Temperature Detectors, Madison, WI, July 2001.

[20] K.D. Irwin, G.C. Hilton, D.A. Wollman, J.M. Martinis, J. Appl. Phys. 83 (1998) 3978.

[21] Elston, R. (ed), "Astrophysics with IR-Arrays," Astronom. Soc. Of the Pacific Conference Series, San Francisco, vol. 15, 1991.

[22] D. A. Wollman, K. D. Irwin, G. C. Hilton, L. L. Dulcie, D. E. Newbury, J. M. Martinis, J. Microsc. 188 (1977) 196.